Spin transport study in a disordered-metal/ferromagnetic-insulator heterostructure based on full counting statistics within the coherent potential approximation

Gaoyang Li[1] and Jian Wang[1,2,*]

[1]*College of Physics and Optoelectronic Engineering, Shenzhen University, Shenzhen 518060, China*

[2]*Department of Physics, The University of Hong Kong, Pokfulam Road, Hong Kong, China*

(Received 6 May 2023; accepted 13 February 2024; published 4 March 2024)

We present a theoretical formalism to investigate quantum spin transport in a two-dimensional metal/ferromagnetic insulator (FI) heterostructure in the presence of disorder. The formalism is based on the full counting statistics (FCS) within coherent potential approximation (CPA), which is capable of calculating the disorder average of an arbitrary number of Green's functions. Due to the convolutional structure of the self-energy of the FI lead, the conventional FCS-CPA formalism breaks down in our system. We propose two solutions to solve this problem. We numerically examine the formalism by calculating the average spin conductance in a disordered nonmagnetic metal/FI (NM/FI) heterostructure and apply it to a disordered altermagnetic metal/FI (AM/FI) heterostructure. The FCS-CPA results exhibit excellent agreement with brute force calculations in weak disorders. In AM/FI systems, the spin transport is enhanced in weak disorders and suppressed in strong disorders. Stronger anisotropic hopping suppresses the spin transport in AM/FI systems. The average spin conductance is notably sensitive to the spin polarization of AM states. The methods proposed here are also applicable to the convolutional self-energy in electron-phonon coupling systems.

DOI: 10.1103/PhysRevB.109.125403

I. INTRODUCTION

Spin transport is a major subject of spintronics. Electronic and magnonic spin currents are its two main components [1–6]. The electronic spin current is usually generated in a nonmagnetic metal (NM) via the spin Hall effect [5,7–9] or at the interface of a ferromagnet and a normal metal via the spin pumping effect [10–14]. Due to various scattering processes from phonons, electrons, and defects, the electronic spin current usually decays over short distances and produces inevitable Joule heat. In ferromagnetic insulators (FIs), conduction electrons are forbidden by the band structure, so the spin current is carried by spin waves or magnons, i.e., magnonic spin current. Since scatterings from conduction electrons are absent, the decay length of magnonic spin current reaches a macroscopic scale of a millimeter [15], and no waste heat is produced. Therefore, magnonic spin current serves as a potential building block of the next-generation computing platform. Since the infrastructure of conventional electronic devices is well developed and has several advantages, a feasible option is to integrate magnonics into the existing electronic architectures, among which the NM/FI bilayer structure is widely used in theoretical and experimental investigations [16,17]. Extensive efforts have been made to enhance the spin signals by inserting layers between the NM layer and the FI layer [18–22]. A full quantum theory describing the spin current in an NM/FI heterostructure has been developed [23]. The spin thermoelectric properties of a quantum dot connected to magnetic insulator and metal electrodes in the presence of Coulomb repulsion has also been investigated [24].

Recently, a unique magnetic phase termed altermagnetism has been reported in ruthenium dioxide (RuO_2) [25–27], where two sublattices with opposite spins result in anisotropic spin-splitting with a magnitude of eV scale in reciprocal space [28]. The spin-splitting alternates in sign across the band structure. Notably, it has been demonstrated that a strong transverse spin current can be generated, akin to the spin Hall effect, by applying an external electric field, even in the absence of the relativistic spin-orbit coupling [29–31]. Altermagnets have significantly broadened the material landscape for spintronics [32–36]. While the transport across junctions of altermagnetic metals (AMs) with normal metals and ferromagnetic metals has been studied [32], there is still a dearth of investigation on spin transport in AM/FI heterostructures.

On the other hand, disorder effects in electronic system have drawn great attention since the pioneering work by Anderson [37]. Various interesting transport phenomena have been uncovered, including weak localization [38–41], weak antilocalization [39,42], Anderson localization [37], and universal conductance fluctuation [43–47]. Numerically, transport properties can be studied using the Landauer-Büttiker formula in the nonequilibrium Green's function framework. Despite the success of numerical investigations in various electronic systems, the vast computational cost remains a big challenge. To obtain an accurate estimation of a disorder-averaged physical quantity, the quantity must be calculated for a large number of disorder samples. This is called the brute force calculation. To reduce the computational cost of brute force calculation, a number of approximated schemes were developed [48–58]. The coherent potential approximation [48–51] (CPA) was introduced to calculate the disorder average of a single retarded Green's function $\langle G^r \rangle$, from which we can obtain the density of states

*jianwang@hku.hk

 ©2024 American Physical Society

(DOS) of the disordered system. The nonequilibrium vertex correction (NVC) method [52–55] was invented to deal with the transmission coefficient, which involves the production of two Green's functions. A generalized nonequilibrium vertex correction (GNVC) method [56,57] was proposed to solve the disorder average of four Green's functions, which can be used to calculate the average conductance fluctuation and shot noise. As a powerful approach, the full counting statistic method within CPA (FCS-CPA) is capable of solving the average of an arbitrary number of Green's functions [58]. Moreover, the FCS-CPA method has proven to be powerful in charge and phonon transport studies [58,59]. However, the existing formalism can not be directly used for spin transport studies, especially for spin current mediated by magnon in disordered systems such as NM/FI and AM/FI hybrid systems.

In this paper, we extend the FCS-CPA formalism to the spin transport study in metal/ferromagnetic insulator (M/FI) hybrid systems, such as the NM/FI system and AM/FI system. Conventional FCS-CPA formalism in studying charge conductance in NM systems relies on an important property of the cumulant generating function (CGF), i.e., the disorder in CGF is completely included in the Green's functions, and there should be no disorder in self-energies. However, this property is no longer respected in M/FI system and the self-energy is expressed as the convolution of Green's function of scattering region and the bare self-energy of the FI lead because of the third-order interaction between the electron and magnon. Due to the convolutional structure of self-energy, disorder enters the self-energy through the Green's function of the central scattering region. The conventional FCS-CPA formalism thus breaks down. We propose two solutions to address this problem within the conventional FCS-CPA formalism. Subsequently, we apply our methods to numerically investigate the spin transport in disordered NM/FI and AM/FI heterostructures. In the NM/FI system, it is found that in weak disorders, FCS-CPA gives accurate estimations for average spin conductance. While in strong disorders, the results deviate from brute force calculation due to the CPA approximation. Additionally, in the AM/FI system, the enhancement in spin conductance in weak disorders is also observed. Stronger anisotropic hopping t_J tends to facilitate the suppression of spin transport by disorder. The disorder-averaged spin conductance displays a pronounced angle dependence, serving as a key signature of altermagnets.

The rest of the paper is organized as follows. In Sec. II, we first introduce our model and the spin current formula in the Born approximation (BA). Then we generalize the conventional FCS-CPA formalism to calculate spin conductance in M/FI hybrid system and propose two approximate methods to deal with the convolutional self-energy due to the electron-magnon interaction. In Sec. III, we apply our method to investigate the spin transport in a disordered NM/FI heterostructure and a disordered AM/FI heterostructure. Section IV is our conclusion part.

II. MODEL AND THEORETICAL FORMALISM

In this section, we introduce our model and outline the previously obtained spin current formula in the DC case [23].

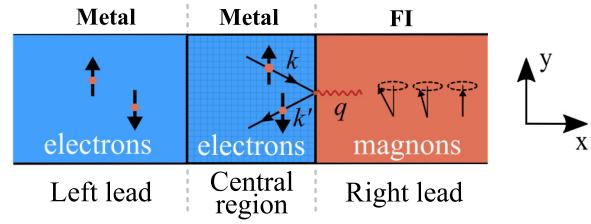

FIG. 1. Schematic view of the 2D M/M/FI system in consideration. A metal lead and an FI lead are connected to a central metallic scattering area. In numerical calculations, Anderson-type disorder is added on the central scattering region. The x direction is the transport direction.

Then we briefly review procedures in conventional FCS-CPA formalism and generalize it to M/FI hybrid systems.

A. Model Hamiltonian and spin current formula

The M/M/FI heterostructure considered in this paper is schematically illustrated in Fig. 1, where a central metallic region is connected to a left metallic lead and a right FI lead. The whole structure Hamiltonian is written as ($e = 1$ and $\hbar = 1$)

$$H = H_{\text{center}} + H_{\text{leads}} + H_{\text{coupling}}. \tag{1}$$

The first two terms describe the Hamiltonians of center region (H_{center}) and isolated leads (H_{leads}), with

$$H_{\text{center}} = \sum_{n\sigma} (\varepsilon_{n\sigma} + V) d^{\dagger}_{n\sigma} d_{n\sigma} \tag{2}$$

and

$$H_{\text{leads}} = H_L + H_R. \tag{3}$$

Here $d^{\dagger}_{n\sigma}$ is the creation operator of electrons in the central region. In the presence of disorder, a random potential V is added to the on-site potential $\varepsilon_{n\sigma}$. $H_L = \sum_{k\sigma} (\varepsilon_{k\sigma} - \mu_{L\sigma}) c^{\dagger}_{k\sigma} c_{k\sigma}$ is the Hamiltonian of the left metallic lead, which is described by free electrons. Here $c^{\dagger}_{k\sigma}$ creates an electron with momentum k and spin σ in the left lead. $\mu_{L\sigma}$ is the spin-dependent chemical potential of electrons injected from the left lead. The right FI lead could be described by the Heisenberg model, which under Holstein-Primakoff transformation [60] and the linear spin-wave approximation [61] reduces to free magnons [62] described by $H_R \approx \sum_q \omega_q a^{\dagger}_q a_q$. Operator $a^{\dagger}_q (a_q)$ creates (annihilates) a magnon with momentum q. The magnon dispersion ω_q is given by material details.

The coupling Hamiltonian between the central region and two leads is

$$H_{\text{coupling}} = H_{\text{T}} + H_{\text{sd}}, \tag{4}$$

with

$$H_{\text{T}} = \sum_{k\sigma n} [t_{k\sigma n} c^{\dagger}_{k\sigma} d_{n\sigma} + t^{*}_{k\sigma n} d^{\dagger}_{n\sigma} c_{k\sigma}] \tag{5}$$

and

$$H_{\text{sd}} = -\sum_{qnn'} J_{qnn'} [d^{\dagger}_{n\uparrow} d_{n'\downarrow} a^{\dagger}_q + d^{\dagger}_{n'\downarrow} d_{n\uparrow} a_q]. \tag{6}$$

Here $H_{\rm T}$ describes the electronic hopping between the left lead and the central region. $H_{\rm sd}$ is the coupling between electrons in the central metallic region and magnons in the right FI lead, which is described by the so-called sd exchange interaction. $J_{qnn'}$ is the scattering strength of the process where an electron in level n' with spin σ is scattered to level n with spin $\bar{\sigma}$ while absorbing or emitting a magnon.

In the presence of a temperature gradient ΔT between the left and right lead or a spin voltage $\mu_s = \mu_{L\uparrow} - \mu_{L\downarrow}$, a pure spin current flows through the heterostructure due to the longitudinal spin Seebeck effect [16,17]. After performing the perturbation expansion in the nonequilibrium Green's function formalism, we obtained the pure spin current I_s in the heterostructure [23]. In the DC case, the spin current is given by

$$I_s = -\int dE \mathrm{Tr}[G^r_\uparrow(E)\Gamma_{L\uparrow}(E)G^a_\uparrow(E)\bar{\Gamma}_{R\uparrow}(E)]. \tag{7}$$

The Green's function $G^{r,a}_\uparrow$ is defined as

$$G^{r,a}_\uparrow(E) = \frac{1}{E - H - \Sigma^{r,a}_{L\uparrow}(E) - \bar{\Sigma}^{r,a}_{R\uparrow}(E)}, \tag{8}$$

and $\Gamma_{L\uparrow}(E) = -2\mathrm{Im}\Sigma^r_{L\uparrow}(E)$ is the linewidth function of the left lead, where $\Sigma^r_{L\uparrow}$ is the self-energy of left metallic lead. The effective self-energy of the right FI lead is formulated as

$$\bar{\Sigma}^r_{R\uparrow}(E) = \int \frac{d\omega}{2\pi}\big[f_R(\omega)G^r_{L\downarrow}(\bar{E}) + if_{L\downarrow}(\bar{E})\mathrm{Im}G^r_{L\downarrow}(\bar{E})\big]\Gamma_R(\omega), \tag{9}$$

which is an energy convolution of local partial DOS with the spectral function of FI lead. Here we define $\bar{E} = E + \omega$. $G^{r,a}_{L\downarrow}$ is the Green's function when central region is connected to left lead only, which is defined as

$$G^{r,a}_{L\downarrow}(\bar{E}) = \frac{1}{\bar{E} - H - \Sigma^{r,a}_{L\downarrow}(\bar{E})}. \tag{10}$$

We note that the effective self-energy of the right FI lead here is a key quantity in M/FI system. It makes the enhancement of spin current by manipulating interfacial potentials possible [23], which provides insight into amplifying SSE signals. Inthe BA, the effective linewidth function of the right lead is given by

$$\bar{\Gamma}_{R\uparrow}(E) = i\bar{\Sigma}^<_{R\uparrow}(E) - 2f_{L\uparrow}(E)\mathrm{Im}\bar{\Sigma}^r_{R\uparrow}(E), \tag{11}$$

with

$$\bar{\Sigma}^<_{R\uparrow}(E) = i\int d\omega\left(\frac{1}{2} + f^B_R(\omega)\right)f_{L\downarrow}(\bar{E})D^0_{L\downarrow}(\bar{E})\Gamma_R(\omega), \tag{12}$$

in which $f^B_R(\omega) = 1/[\exp(\beta_R\omega) - 1]$ is the Bose-Einstein distribution for the right magnonic lead, $f_{L\sigma}(E) = 1/[\exp(\beta_L(E - \mu_{L\sigma})) + 1]$ is the Fermi-Dirac distribution for the left electronic lead, and $f^B_L(\omega) = 1/[\exp(\beta_L\omega + \mu_s) - 1]$ is an effective Bose-Einstein distribution for the left Fermion lead [23]. $\beta_L = 1/k_BT_L$ and $\beta_R = 1/k_BT_R$ are the inverse temperatures of the left and right leads. $D^0_{L\downarrow}(E) = G^r_{L\downarrow}(E)\Gamma_{L\downarrow}(E)G^a_{L\downarrow}(E)$ is the injectivity from the left lead, $\Gamma_R = i(\Sigma^r_R - \Sigma^a_R)$ is the linewidth function of right magnonic lead. We can see that self-energies, thus the effective linewidth function of the right lead, is disorder-dependent due to the convolution of the central region Green's functions in self-energy expression.

In the linear-response regime, the spin current can be expressed as

$$I_s = G_T\Delta T - G_\mu\mu_s, \tag{13}$$

with G_T and G_μ the linear-response coefficients in small temperature difference ΔT and spin voltage μ_s. Coefficients G_T and G_μ characterize the ability the heterostructure transports the spin flow. We call them spin conductance driven by temperature gradient and spin conductance driven by spin bias, respectively.

B. FCS-CPA formalism in M/FI system

For electronic transport studies in the presence of Anderson disorder, an on-site potential V_i is added on each lattice site i. Here V_i is a random energy chosen from a box distribution in the range of $[-W/2, W/2]$, where W is the disorder strength. To obtain an accurate estimate of the disorder average of a transport quantity, one must collect a large number of disorder samples for a specific disorder strength. This can be quite time-consuming for large or interacting systems. By using a dimension expansion, the FCS-CPA formalism maps the nonlinear functional dependence of the generating function on multiple Green's functions into a linear dependence on the dimension-expanded Green's function, avoiding the complicated diagrammatic expansion operation [63–67]. All high-order cumulants can thus be evaluated through the average of the dimension-expanded Green's function in CPA. In this sense, the FCS-CPA formalism has made significant progress in reducing computational costs.

In this subsection, we demonstrate that spin transport in M/FI systems can also be formulated using the FCS-CPA formalism. We begin with the most important quantity in the FCS-CPA formalism, the CGF. Similar to the CGF for charge conductance in normal metal systems, the CGF for spin current in M/FI is given by

$$\ln\mathcal{Z} = \mathrm{Tr}\ln[I + \hat{T}(e^\kappa - 1)], \tag{14}$$

where κ is the counting field [58] and $\hat{T}$ is the operator to be averaged for different disorder samples. The nth cumulant C_n of operator $\hat{T}$ can be calculated by taking the nth derivative of $\ln\mathcal{Z}$ with respect to κ at $\kappa = 0$. For instance, the first and second cumulants of $\hat{T}$ can be readily verified as

$$C_1 = \mathrm{Tr}(\hat{T}) = \left.\frac{\partial\ln\mathcal{Z}}{\partial\kappa}\right|_{\kappa=0}, \tag{15}$$

$$C_2 = \mathrm{Tr}(\hat{T} - \hat{T}^2) = \left.\frac{\partial^2\ln\mathcal{Z}}{\partial\kappa^2}\right|_{\kappa=0}. \tag{16}$$

In the presence of disorder, the average of cumulants C_n is equal to the nth derivative of the disorder-averaged CGF

$$\langle C_n\rangle = \left.\frac{\partial^n\langle\ln\mathcal{Z}\rangle}{\partial\kappa^n}\right|_{\kappa=0}, \tag{17}$$

where $\langle\cdots\rangle$ denotes the disorder average on a physical quantity. For charge-transport studies in normal metal systems, $\hat{T} = \Gamma_L G^r\Gamma_R G^a$ naturally relates C_1 and C_2 to the charge conductance and conductance fluctuation. To formulate the spin current Eq. (7) in FCS-CPA formalism, we define

$$\hat{T} = G^r_\uparrow(E)\Gamma_{L\uparrow}(E)G^a_\uparrow(E)\bar{\Gamma}_{R\uparrow}(E). \tag{18}$$

Then the spin current for a clean system can be expressed by the CGF as

$$I_s = -\int dE C_1 = -\int dE \left.\frac{\partial \ln \mathcal{Z}}{\partial \kappa}\right|_{\kappa=0}. \tag{19}$$

The disorder average of the first-order cumulant gives the spin current average:

$$\langle I_s\rangle = -\int dE \left.\frac{\partial \langle \ln \mathcal{Z}\rangle}{\partial \kappa}\right|_{\kappa=0}. \tag{20}$$

In the following, we will take Eq. (18) as an example to illustrate the procedures in FCS-CPA formalism. Since the Green's functions and linewidth functions share the same variable E, we will omit the E dependence for convenience. The FCS-CPA formalism discussed below transforms the multi-Green's functions in $\hat{T}$ to a single dimension-expanded Green's function, whose disorder average can be further solved within CPA. Note that the CGF in Eq. (14) can be reformulated as

$$\ln \mathcal{Z} = \mathrm{Tr}\left[\int_0^\zeta dx \mathcal{G}(x) M\right], \tag{21}$$

with

$$\mathcal{G}(x) = \frac{1}{G^{-1} + Mx}, \tag{22}$$

where G is the dimension-expanded Green's function and $\zeta = \sqrt{e^\kappa - 1}$. G and M are defined as

$$G = \begin{pmatrix} G^r_\uparrow & 0 \\ 0 & G^a_\uparrow \end{pmatrix}, \tag{23}$$

$$M = \begin{pmatrix} 0 & -\Gamma_{L\uparrow} \\ \bar{\Gamma}_{R\uparrow} & 0 \end{pmatrix}, \tag{24}$$

in which the Green's function $G^{r,a}_\uparrow$ and linewidth function $\bar{\Gamma}_{R\uparrow}$ are defined in Eqs. (8) and (11), respectively. In the dimension expansion of the Green's function, the equality $\ln \mathrm{Det}\, X = \mathrm{Tr} \ln X$ for matrix X is used [58]. The matrix design of G and M for a specific operator $\hat{T}$ is a key step in implementing the FCS-CPA formalism.

If matrix M is independent of the disorder sample, the disorder average of the CGF can be expressed as

$$\langle \ln \mathcal{Z}\rangle = \mathrm{Tr}\left[\int_0^\zeta dx \langle \mathcal{G}(x)\rangle M\right]. \tag{25}$$

However, this assumption does not hold in our system. Despite this, we will illustrate the main procedures of the FCS-CPA formalism assuming that the above equation is valid. We will discuss the difficulty brought in by the disorder-dependent M and how to overcome it at the end of this subsection. The averaged Green's function $\langle \mathcal{G}(x)\rangle$ can be evaluated within the CPA approach [58]. In CPA, the disorder effect on the Green's function is collected in an effective potential matrix V,

$$\langle \mathcal{G}(x)\rangle = \frac{1}{G^{-1} + Mx - V}, \tag{26}$$

$$V = \begin{pmatrix} V_{11} & V_{12} \\ V_{21} & V_{22} \end{pmatrix}. \tag{27}$$

To obtain a closed equation for V, the single-site approximation (SSA) is commonly used, in which the contribution of multiple scatterings from the same sites is neglected [58]. However, this approximation can lead to large errors when local resonances or bound states exist in the system [68]. In the SSA, $V_{\alpha\beta}$ is a diagonal subblock matrix of V. Alternatively, the effective on-site potential of site i for CGF can be expressed as

$$V^{ii} = \begin{pmatrix} V^{ii}_{11} & V^{ii}_{12} \\ V^{ii}_{21} & V^{ii}_{22} \end{pmatrix}, \tag{28}$$

which satisfies the CPA self-consistent equation

$$V^{ii} = \int dv^{ii} \rho(v^{ii}) v^{ii} [I - \langle \mathcal{G}(x)\rangle^{ii} (v^{ii} I - V^{ii})]^{-1}. \tag{29}$$

Here $\rho(v^{ii})$ is the distribution function of disorder strength v at site i. For the Anderson-type disorder:

$$\rho(v^{ii}) = \begin{cases} 1/W, & -W/2 \leqslant v^{ii} \leqslant W/2 \\ 0, & \text{otherwise.} \end{cases} \tag{30}$$

Converging the effective potential matrix V self-consistently and substituting these equations into Eq. (20), we finally obtain the average spin current in FCS-CPA formalism in the small ζ limit:

$$\langle I_s\rangle = \frac{1}{2\zeta} \int dE\, \mathrm{Tr}\,[\langle \mathcal{G}(\zeta)\rangle M]. \tag{31}$$

Note it has been shown [58] that in the limit of $\zeta = 0$, $\mathrm{Tr}[\langle \mathcal{G}(\zeta)\rangle M]/\zeta$ is finite.

We note in Eq. (25) that for normal metal systems the matrix M is independent of disorder. This property ensures that the disorder average of CGF reduces to the disorder average of a single Green's function, which can be further evaluated in CPA. However, this property is not respected in our M/FI system due to the energy convolution in $\bar{\Gamma}_{R\uparrow}$ and $\bar{\Sigma}^r_{R\uparrow}$. This convolutional structure presents a major challenge in solving this model within the FCS-CPA formalism. Since the self-energy in electron-phonon coupling system has a similar convolutional structure, we expect the same problem to arise when applying the FCS-CPA formalism to electron-phonon interacting system.

1. J^2 approximation

To avoid the disorder-dependent matrix M in Eq. (25), we propose two solutions in this paper. One intuitive idea is to eliminate the energy convolution. If we keep the spin current in only J_q^2 order, there will be no $\bar{\Sigma}^r_{R\uparrow}$ dependence in the Green's functions since Γ_R is proportional to J_q^2 already [see Eq. (41)]. This is a stronger approximation than the BA. We denote this approximation as the J^2 approximation, which has been used in other studies [69–71]. In the J^2 approximation, the spin current formula Eq. (7) reduces to

$$I_s = -\int \frac{d\omega}{2\pi} [f^B_R(\omega) - f^B_L(\omega)] \int dE [f_{L\uparrow}(E) - f_{L\downarrow}(E+\omega)] \mathrm{Tr} A(E,\omega), \tag{32}$$

with

$$A = D^0_{L\uparrow}(E)D^0_{L\downarrow}(\bar{E})\Gamma_R(\omega). \tag{33}$$

In carrying out FCS-CPA in the J^2 approximation, the $\hat{T}$ operator in Eq. (14) is denoted as $\hat{T}_1$:

$$\hat{T}_1 = A = D^0_{L\uparrow}(E)D^0_{L\downarrow}(\bar{E})\Gamma_R(\omega). \tag{34}$$

For Eq. (34), there are four Green's functions in operator $\hat{T}_1$. The formalism introduced above is still valid in this case, but with a different construction of matrices G and M. For $\hat{T}_1$, we have

$$G = \begin{pmatrix} G^r_{L\uparrow}(E) & 0 & 0 & 0 \\ 0 & G^r_{L\uparrow}(\bar{E}) & 0 & 0 \\ 0 & 0 & G^a_{L\uparrow}(\bar{E}) & 0 \\ 0 & 0 & 0 & G^a_{L\uparrow}(E) \end{pmatrix}, \tag{35}$$

$$M = \begin{pmatrix} 0 & 0 & 0 & \Gamma_{L\uparrow}(E) \\ 0 & 0 & -\Gamma_{L\uparrow}(\bar{E}) & 0 \\ \Gamma_R(\omega) & 0 & 0 & 0 \\ 0 & \mathcal{I} & 0 & 0 \end{pmatrix}, \tag{36}$$

where the $\mathcal{I}$ is a unit matrix of the same size as Γ_R. The average spin current is thus given by

$$\langle I_s\rangle = -\frac{1}{4\zeta^3}\int\frac{d\omega}{2\pi}\left(f^B_R(\omega) - f^B_L(\omega)\right)\int\frac{dE}{2\pi}(f_L(E) - f_L(E+\omega))\,\mathrm{Tr}\,[\langle\mathcal{G}(\zeta)\rangle M], \tag{37}$$

with $\zeta = (e^{\kappa} - 1)^{1/4}$ in this case. Again, in the limit of $\zeta = 0$, $\mathrm{Tr}[\langle\mathcal{G}(\zeta)\rangle M]/\zeta^3$ converges.

2. Mean-field approximation

The other solution is to make a mean-field-like approximation on top of the BA. We assume $\bar{\Gamma}_{R\uparrow}$ in matrix M to be independent of disorder samples by replacing it with its disorder-average $\langle\bar{\Gamma}_{R\uparrow}\rangle$. We denote the operator $\hat{T}$ in this approximation as

$$\hat{T}_2 = G^r_{\uparrow}(E)\Gamma_{L\uparrow}(E)G^a_{\uparrow}(E)\langle\bar{\Gamma}_{R\uparrow}(E)\rangle. \tag{38}$$

In this approximation, the disorder average of the CGF becomes

$$\langle\ln\mathcal{Z}\rangle = \mathrm{Tr}\left[\int_0^{\zeta} dx\langle\mathcal{G}(x)\rangle\tilde{M}\right], \tag{39}$$

with

$$\tilde{M} = \begin{pmatrix} 0 & -\Gamma_{L\uparrow} \\ \langle\bar{\Gamma}_{R\uparrow}\rangle & 0 \end{pmatrix}, \tag{40}$$

in which, $\langle\bar{\Gamma}_{R\uparrow}\rangle$ is prepared by CPA calculation in advance. The dimension-expanded Green's function $\mathcal{G}(x)$ is the same as Eq. (23).

III. NUMERICAL RESULTS AND DISCUSSION

In this section, we present FCS-CPA results on the average spin conductance in the two approaches proposed above. We first demonstrate the performance of FCS-CPA by comparing it with BF results in an NM/FI heterostructure under the J^2 approximation and mean-field approximation, and then use it to investigate the spin transport in a disordered AM/FI heterostructure under J^2 approximation.

The central scattering region consists of a two-dimensional square lattice with a size of $20a \times 20a$. The effect of the left NM lead on the central scattering region is taken into account by the self-energy, which is calculated from the transfer-matrix method [72]. The coupling between the right FI lead and the central scattering region is modeled by an Ohmic linewidth function

$$\Gamma_R(\omega) = \alpha\omega e^{-\omega/\omega_c}t\Gamma_0, \tag{41}$$

where $\alpha \sim J_q^2$ is the dimensionless effective coupling strength. As discussed in Ref. [73], α is related to the spin mixing conductance [10,74]. ω_c is the cutoff frequency used to truncate the Ohmic spectrum in high frequency. Γ_0 is a unit matrix with nonzero elements at the NM/FI interface. This Γ_0 assumes that the scattering between electrons and magnons only occurs at the interface, as used by other studies [69–71]. Other choices of Γ_R will not change the results qualitatively. In numerical calculations, we choose $\alpha = 100$.

In the linear-response regime, a small temperature bias ΔT is applied symmetrically to the two leads, or a small spin voltage μ_s is introduced in the left NM lead. The spin conductance G_T is evaluated by setting $\mu_s = 0$, while the spin conductance G_μ is evaluated by setting $\Delta T = 0$.

A. FCS-CPA in J^2 approximation in NM/FI heterostructure

In the NM/FI heterostructure, we set the lattice constant $a = 5$ nm, resulting in a hopping constant of $t = 21.768$meV in tight-binding calculations. The temperature of the heterostructure is set to $T = 5$K and the chemical potential of the left NM lead is set to $\mu_L = 0.9$ meV, with the chemical potential of the right FI lead as the reference point. The cutoff frequency in the magnon spectrum is set to $\omega_c = 0.24$ meV. These parameters set the entire scattering process in the first subband. The transport behaviors in the second subband are qualitatively similar to those in the first subband [75].

In the J^2 approximation, Eq. (34) is used. To reduce the computational cost, we have used the relation $G^r_{L\sigma}\Gamma_{L\sigma}G^a_{L\sigma} = i(G^r_{L\sigma} - G^a_{L\sigma})$, then the operator $\hat{T}_1$ is simplified to

$$\hat{T}_1 = -G^r_{L\uparrow}(E)G^r_{L\downarrow}(\bar{E})\Gamma_R(\omega) + G^r_{L\uparrow}(E)G^a_{L\downarrow}(\bar{E})\Gamma_R(\omega) + G^a_{L\uparrow}(E)G^r_{L\downarrow}(\bar{E})\Gamma_R(\omega) - G^a_{L\uparrow}(E)G^a_{L\downarrow}(\bar{E})\Gamma_R(\omega). \tag{42}$$

We substitute the above $\hat{T}_1$ into Eq. (32) and perform double integration using both brute force and FCS-CPA methods. For brute force calculations, we collect 60 000 disorder samples to smooth out the average spin conductance curve. For FCS-CPA calculations, we use similar matrix constructions as shown in Eqs. (23) and (24). For example, the matrix constructions for the first term $G^r_{L\uparrow}(E)G^r_{L\downarrow}(\bar{E})\Gamma_R(\omega)$ in the above $\hat{T}_1$ are

$$G = \begin{pmatrix} G^r_{L\uparrow}(E) & 0 \\ 0 & G^r_{L\downarrow}(\bar{E}) \end{pmatrix}, \tag{43}$$

$$M = \begin{pmatrix} 0 & \mathcal{I} \\ -\Gamma_R(\omega) & 0 \end{pmatrix}. \tag{44}$$

The results are shown in Fig. 2. In Fig. 2(a), we plot the average spin conductance $\langle G_T\rangle$ for a wide range of disorder strength. $\langle G_T\rangle$ in the J^2 approximation exhibits a

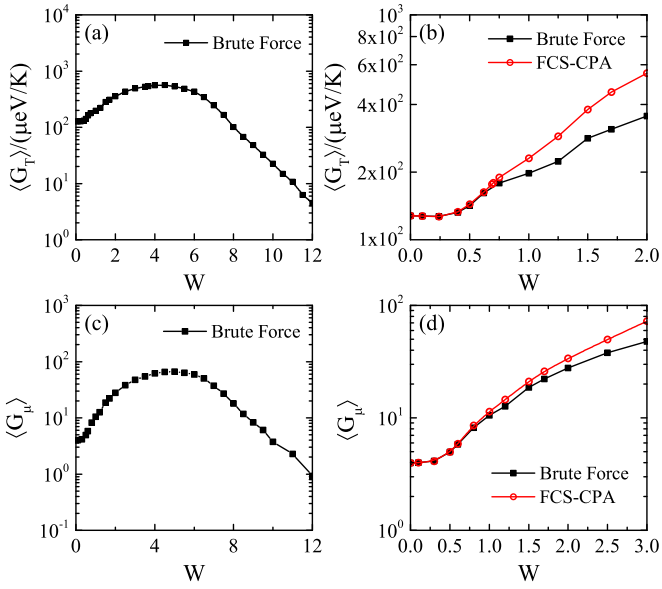

FIG. 2. The average spin conductance $\langle G_T \rangle$ and $\langle G_\mu \rangle$ as a function of disorder strength W in units of hopping constant t for brute force and FCS-CPA calculation in J^2 approximation. Sixty-thousand disorder samples are collected for brute force calculation. (a), (b) The spin conductance $\langle G_T \rangle$. (c)–(d) The spin conductance $\langle G_\mu \rangle$.

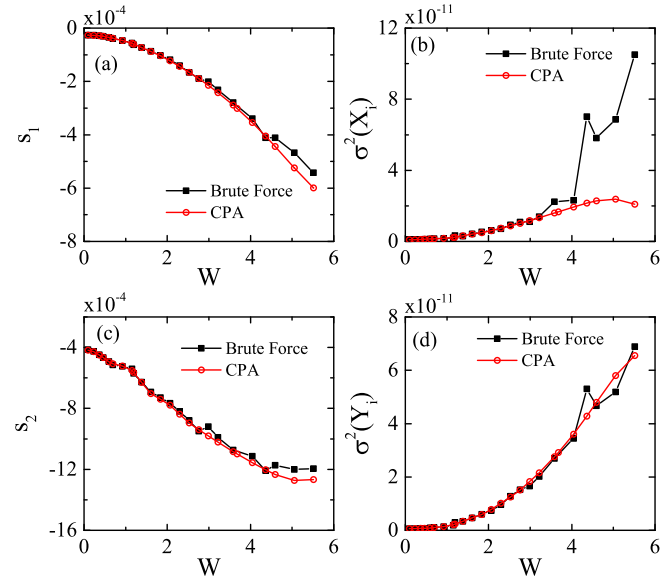

FIG. 3. Brute force and CPA calculations for $\langle \bar{\Gamma}_{R\uparrow} \rangle$ as a function of disorder strength. (a), (b) The summation and variance of diagonal elements of the disorder-averaged matrix $\langle \bar{\Gamma}_{R\uparrow} \rangle$ obtained from brute force calculation (black box) and CPA approximation (red circle). (c), (d) The summation and variance of off-diagonal elements of the disorder-averaged matrix $\langle \bar{\Gamma}_{R\uparrow} \rangle$.

nonmonotonic dependence on disorder strength W, which is also found in the BA [75]. It was found that this nonmonotonic behavior is the consequence of competition between disorder-enhanced DOS at NM/FI interface and Anderson localization [75]. In weak disorders, the interfacial DOS is enhanced due to potential dips introduced by disorders. The convolution of enhanced interfacial DOS in turn enhances the spin conductance. In strong disorders, the localization of electrons in central region blocks the spin transport.

In the strong disorder regime, the linear dependence in a log plot suggests that in this regime the electron is localized [76]. Since the J^2 approximation neglects the right self-energy in the denominator of Green's functions, the evaluated average spin conductance is much larger than that in BA [75]. In Fig. 2(b), we compare the brute force and FCS-CPA results. In weak disorders, the FCS-CPA result agrees well with the brute force calculation. However, for disorder strength $W > 0.7$, FCS-CPA starts to overestimate the average spin conductance $\langle G_T \rangle$. We also calculate in Fig. 2(c) the spin conductance $\langle G_\mu \rangle$ driven by a spin voltage using the brute force method. The curve shows similar nonmonotonic behavior. Finally, in Fig. 2(d), we compare results of spin conductance $\langle G_\mu \rangle$ in brute force and FCS-CPA methods. The FCS-CPA is accurate for $W < 0.8$. Moreover, for stronger disorder $W \sim 2$, FCS-CPA also gives fair estimation to $\langle G_\mu \rangle$.

We note that the deviation from brute force calculation in larger disorders is due to nature of CPA method, which is present in all CPA-related approaches. As mentioned in Sec. II B, SSA is used to obtain a closed form equation for the effective potential V. This approximation works well in weak disorders. While in strong disorders, multiple scattering events are expected to play important roles. The failure of SSA leads to the deviation of FCS-CPA results. Additionally, this overestimation behavior in larger disorders is also observed in electron and phonon transport studies [58,59].

B. FCS-CPA in mean-field approximation in NM/FI heterostructure

As mentioned earlier, the J^2 approximation is a strong approximation that completely ignores the effective right self-energy considered in BA. For FCS-CPA calculation in the mean-field approximation, we start with $\hat{T}_2$ and decouple the disorder correlation between Green's functions and self-energies by replacing $\bar{\Gamma}_{R\uparrow}$ with its average $\langle \bar{\Gamma}_{R\uparrow} \rangle$.

We first prepare the disorder average $\langle \bar{\Gamma}_{R\uparrow} \rangle$ in matrix $\tilde{M}$ defined in Eq. (40). By using $D^0_{L\downarrow} = -2\mathrm{Im}G^r_{L\downarrow}$, we have

$$\langle \bar{\Sigma}^<_{R\uparrow}(E) \rangle = -2i \int d\omega \left(\frac{1}{2} + f^B_R(\omega) \right) f_{L\downarrow}(\bar{E}) \mathrm{Im}\langle G^r_{L\downarrow}(\bar{E}) \rangle \Gamma_R(\omega) \tag{45}$$

and

$$\langle \bar{\Sigma}^r_{R\uparrow}(E) \rangle = \int \frac{d\omega}{2\pi} \big[f_R(\omega) \langle G^r_{L\downarrow}(\bar{E}) \rangle + i f_{L\downarrow}(\bar{E}) \mathrm{Im}\langle G^r_{L\downarrow}(\bar{E}) \rangle \big] \Gamma_R(\omega). \tag{46}$$

From Eq. (11), the calculation of disorder average $\langle \bar{\Gamma}_{R\uparrow} \rangle$ reduces to the disorder average $\langle G^r_{L\downarrow} \rangle$, which can be further obtained using CPA approximation [58] or brute force calculation.

Figure 3 presents statistics for matrix $\langle \bar{\Gamma}_{R\uparrow} \rangle$ obtained from both the CPA approximation and brute force calculation. Figures 3(a) and 3(b) show the summation and variance of the diagonal elements of the disorder-averaged matrix $\langle \bar{\Gamma}_{R\uparrow} \rangle$. The statistical quantity s_1 is defined as $s_1 = \sum_i X_i$, where

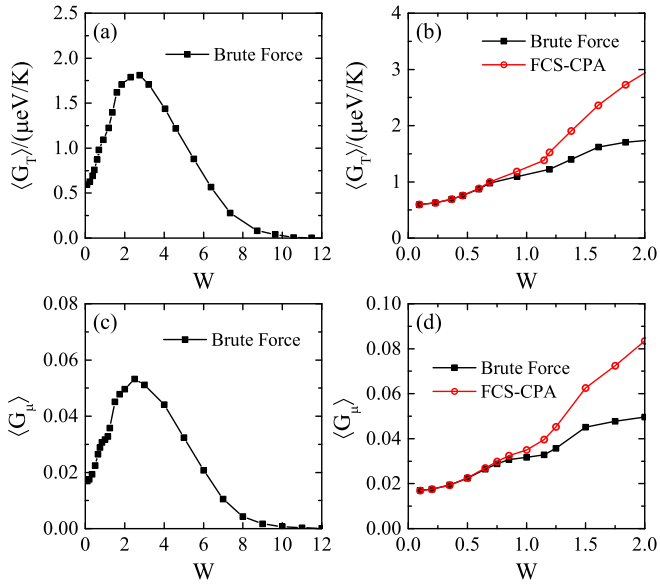

FIG. 4. Brute force and FCS-CPA calculations for average spin conductance $\langle G_T\rangle$ and $\langle G_\mu\rangle$ as a function of disorder strength in mean-field approximation. $\langle\bar{\Gamma}_{R\uparrow}\rangle$ is prepared in advance by CPA calculation. In obtaining average spin conductance, 20000 disorder samples are collected in brute force calculation.

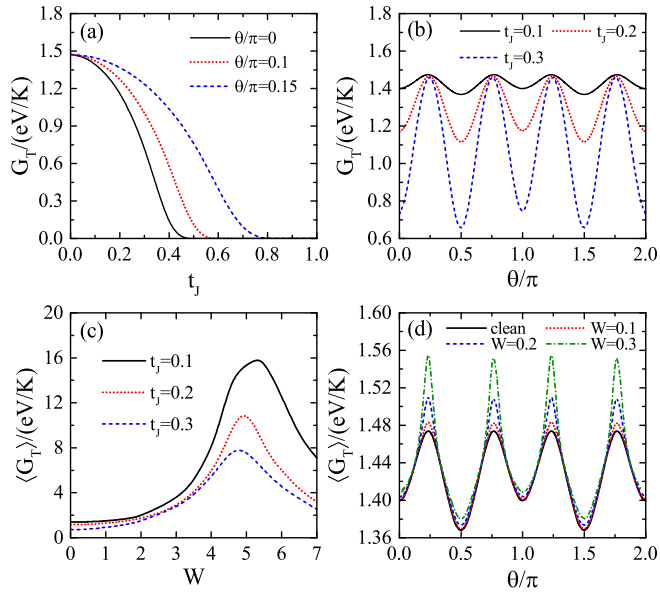

FIG. 5. (a), (b) Spin conductance for clean AM/FI heterostructure for different hopping parameter t_J and angle θ. (c), (d) The average spin conductance of AM/FI heterostructure in the presence of Anderson-type disorder. $\theta = 0$ in (c) and $t_J = 0.1$ in (d). Other parameters: $\mu = 0.9$, $\alpha = 100$, and $\omega_c = 0.012$.

$X_i = [\mathrm{Im}\langle\bar{\Gamma}_{R\uparrow}\rangle]_{ii}$ represents the diagonal elements of the matrix. Figures 3(c) and 3(d) show the same for the off-diagonal elements of the matrix $\langle\bar{\Gamma}_{R\uparrow}\rangle$. The statistical quantity s_2 is defined as $s_2 = \sum_i Y_i$, where $Y_i = [\mathrm{Im}\langle\bar{\Gamma}_{R\uparrow}\rangle]_{jk}$ are the off-diagonal elements of the matrix with indices $j \neq k$. The results are averaged over all discrete energy points used in the spin current integration. Figure 3 indicates that the matrix $\langle\bar{\Gamma}_{R\uparrow}\rangle$ obtained using brute force and CPA are nearly the same over a wide range of disorder strength [0,6]. This allows us to calculate $\langle\bar{\Gamma}_{R\uparrow}\rangle$ using the CPA approximation and develop a formalism that is free from brute force calculation. Note that in previous CPA studies, the interested quantities are scalars. For instance, the conductance, shot noise, etc. Here we verify that CPA is able to accurately describe a matrix, in our case the self-energy of FI lead.

Once $\langle\bar{\Gamma}_{R\uparrow}\rangle$ is obtained, the average spin conductance can be calculated in the same procedures as that of the average electronic transmission in normal metal systems, i.e., Eqs. (22)–(31) with matrix $\tilde{M}$ defined in Eq. (40). As a comparison, the average spin conductance $\langle G_T\rangle$ and $\langle G_\mu\rangle$ are calculated using the brute force method in the mean-field approximation in Fig. 4. In the brute force calculation, we use the same disorder-averaged linewidth function $\langle\bar{\Gamma}_{R\uparrow}\rangle$ obtained earlier. We collect 20000 disorder samples for each disorder strength.

Figures 4(a) and 4(c) show the average spin conductance $\langle G_T\rangle$ and $\langle G_\mu\rangle$ as functions of disorder strength W. We observe that the magnitudes are much smaller compared to those in J^2 approximation. This is due to the consideration of the right self-energy $\bar{\Sigma}^r_{R\uparrow}$ in BA. The nonmonotonic dependence on disorder strength is similar in $\langle G_T\rangle$ and $\langle G_\mu\rangle$. The average spin conductance is enhanced in weak disorders and suppressed in strong disorders. The results are qualitatively similar to brute force results in BA without mean-field approximation [75].

We examine the performance of FCS-CPA in Figs. 4(b) and 4(d). For disorder strength $W < 0.75$, the FCS-CPA formalism gives accurate estimation to $\langle G_T\rangle$ and $\langle G_\mu\rangle$. However, when disorder strength exceeds 0.75, the FCS-CPA begins to overestimate the average spin conductance. Once again, this overestimation is present in all CPA-related studies.

C. FCS-CPA in J^2 approximation in AM/FI heterostructure

In previous subsections, we examined the performance of FCS-CPA. In this subsection, we explore the spin transport in a disordered AM/FI heterostructure using FCS-CPA. The left lead and central region are AMs, whose Hamiltonians are given by [35,36] ($\hbar = e = 2m = 1$)

$$H_{\mathrm{AM}} = \mathbf{k}^2 - \mu + t_1\left(k_x^2 - k_y^2\right)\sigma_z + t_2 k_x k_y \sigma_z. \tag{47}$$

Here, σ_z is the Pauli spin matrix, $\mathbf{k} = (k_x, k_y)$ is the two-dimensional electron momentum, and μ is the Fermi energy. Coupling strengths $t_1 = t_J\cos 2\theta$, $t_2 = t_J \sin\theta\cos\theta$, with t_J the spin-dependent hopping due to the anisotropic exchange interaction in the altermagnetic state. θ parameterizes the angle of the AM/FI interface relative to the crystalline axes. In numerical calculations in AM/FI systems, eV is chosen as the energy unit. We use $\mu = 0.9$, $T = 30$K, and $\omega_c = 0.012$. We present the results of FCS-CPA in the J^2 approximation in Fig. 5.

Figures 5(a) and 5(b) show the spin conductance of a clean AM/FI heterostructure for different coupling strengths t_J and angles θ. For the case of small t_J ($0 < t_J \ll 1$), the Fermi surfaces for up spin and down spin cross each other and enables the spin-flipping process scattered by magnons at AM/FI interface. While for larger t_J, the Fermi surfaces of up

spin and down spin are well separated, resulting in larger spin polarization in central AM region [36]. This, in turn, leads to a smaller spin-flipping rate. Consequently, the spin conductance decreases while increasing t_J. For the Fermi energy $\mu = 0.9$ we used here, only up-spin channels are opened in large t_J, and the spin-flipping scattering is forbidden. Thus the magnon-mediated spin transport vanishes. The spin conductance of the clean AM/FI heterostructure oscillates with θ in the period of π. Moreover, it is symmetric with respect to $\theta = \pi/2$. We observe that the hopping strength t_J suppresses the spin conductance systematically except angles $\theta = \pi/4$ and $3\pi/4$. These angles correspond to $t_1 = 0$ and $t_2 \neq 0$. In this scenario, the system always has zero spin-splitting regardless of the value of t_J [35], thus the spin conductance remains unaffected.

When the Anderson disorder is turned on, we observe in Fig. 5(c) that the spin conductance in AM/FI heterostructure is first enhanced in weak disorders and then suppressed in strong disorders. This behavior is similar to the one in the disordered NM/FI heterostructure [see Fig. 2(a)]. The reason spin conductance got enhanced is that the electron density of states at the AM/FI interface is enhanced by disorder, leading to an increased spin-flipping scattering rate at the interface [75]. In strong disorders, the spin transport is suppressed by Anderson localization of electrons in the central region. Upon increasing anisotropic hopping t_J, the average spin conductance curve is overall suppressed in the same sense that t_J decreases the spin-flipping scattering rate in central region. The maximum suppression occurs at peak position $W \sim 5$. We also note that the FCS-CPA overestimates $\langle G_T \rangle$ at strong disorders according to calculations in NM/FI system.

In Fig. 5(d), we plot the average spin conductance as a function of θ for different disorder strengths W. The anisotropic hopping is chosen as $t_J = 0.1$. We find that the spin conductance enhancement in weak disorders strongly depends on θ. For $\theta = (2n+1)\pi/4$ with integer n, the spin bands of electrons are unpolarized. In this case, the spin transport is significantly enhanced by disorder. While for $\theta = n\pi/2$, the spin polarization of electrons in AM reaches its maximum. We observe that the enhancement is small. Our study indicates that in the AM/FI system, the influence of disorder on the system is closely related to the spin polarization of electrons in AM. When the spin polarization is large, the impact of disorder on the system is minimal. Conversely, when the spin polarization is small, the influence of disorder on the system becomes more significant.

IV. CONCLUSION

In this paper, we developed a theoretical formalism to investigate the magnon mediated spin transport in a 2D M/FI heterostructure. Our theoretical formalism is based on full counting statistics within the CPA. It is capable of calculating the disorder average of an arbitrary number of Green's functions. Due to the convolutional structure of the self-energy of the right magnonic lead in M/FI system, the conventional FCS-CPA formalism breaks down. To address this difficulty, we proposed two solutions, namely, the J^2 approximation and mean-field approximation.

Using brute force method and our FCS-CPA formalism, we have calculated the average spin conductance in the presence of a small temperature difference or a small spin voltage in a disordered NM/FI heterostructure and a disordered AM/FI heterostructure. The numerical results show excellent agreement with brute force calculation in weak disorders. For strong disorders, our formalism overestimates the average spin conductance, which is an inherent flaw of the coherent potential approximation. In addition, the calculations in the AM/FI system show that the spin transport enhancement in weak disorders also exists. The spin-dependent hopping t_J suppresses the spin conductance enhancement and the disorder enhancement depends strongly on spin polarization of AM states. Our study shows that FCS-CPA is suitable for spin transport studies in disordered M/FI heterostructures.

ACKNOWLEDGMENT

This work was financially supported by the Natural Science Foundation of China (Grant No. 12034014).

[1] I. Žutić, J. Fabian, and S. Das Sarma, Rev. Mod. Phys. **76**, 323 (2004).
[2] A. V. Chumak, V. I. Vasyuchka, A. A. Serga, and B. Hillebrands, Nat. Phys. **11**, 453 (2015).
[3] S. A. Wolf, D. D. Awschalom, R. A. Buhrman, J. M. Daughton, S. Von Molnar, M. L. Roukes, A. Y. Chtchelkanova, and D. M. Treger, Science **294**, 1488 (2001).
[4] H. Ohno, Nat. Mater. **9**, 952 (2010).
[5] J. Sinova, S. O. Valenzuela, J. Wunderlich, C. H. Back, and T. Jungwirth, Rev. Mod. Phys. **87**, 1213 (2015).
[6] B. Heinrich, C. Burrowes, E. Montoya, B. Kardasz, E. Girt, Y.-Y. Song, Y. Sun, and M. Wu, Phys. Rev. Lett. **107**, 066604 (2011).
[7] J. E. Hirsch, Phys. Rev. Lett. **83**, 1834 (1999).
[8] S. O. Valenzuela and M. Tinkham, Nature (London) **442**, 176 (2006).
[9] Y. K. Kato, R. C. Myers, A. C. Gossard, and D. D. Awschalom, Science **306**, 1910 (2004).
[10] Y. Tserkovnyak, A. Brataas, and G. E. W. Bauer, Phys. Rev. Lett. **88**, 117601 (2002).
[11] S. Mizukami, Y. Ando, and T. Miyazaki, Phys. Rev. B **66**, 104413 (2002).
[12] E. Saitoh, M. Ueda, H. Miyajima, and G. Tatara, Appl. Phys. Lett. **88**, 182509 (2006).
[13] C. W. Sandweg, Y. Kajiwara, A. V. Chumak, A. A. Serga, V. I. Vasyuchka, M. B. Jungfleisch, E. Saitoh, and B. Hillebrands, Phys. Rev. Lett. **106**, 216601 (2011).
[14] K. Ando, S. Takahashi, J. Ieda, Y. Kajiwara, H. Nakayama, T. Yoshino, K. Harii, Y. Fujikawa, M. Matsuo, S. Maekawa, and E. Saitoh, J. Appl. Phys. **109**, 103913 (2011).
[15] Y. Kajiwara, K. Harii, S. Takahashi, J. Ohe, K. Uchida, M. Mizuguchi, H. Umezawa, H. Kawai, K. Ando, K. Takanashi, S. Maekawa, and E. Saitoh, Nature (London) **464**, 262 (2010).

[16] K. Uchida, H. Adachi, T. Ota, H. Nakayama, S. Maekawa, and E. Saitoh, Appl. Phys. Lett. **97**, 172505 (2010).

[17] K. Uchida, M. Ishida, T. Kikkawa, A. Kirihara, T. Murakami, and E. Saitoh, J. Phys.: Condens. Matter **26**, 389601 (2014).

[18] F. Nakata, T. Niimura, Y. Kurokawa, and H. Yuasa, Jpn. J. Appl. Phys. **58**, 090602 (2019).

[19] Z. Qiu, K. Ando, K. Uchida, Y. Kajiwara, R. Takahashi, H. Nakayama, T. An, Y. Fujikawa, and E. Saitoh, Appl. Phys. Lett. **103**, 092404 (2013).

[20] A. Aqeel, I. J. Vera-Marun, B. J. van Wees, and T. T. M. Palstra, J. Appl. Phys. **116**, 153705 (2014).

[21] F. Hellman, A. Hoffmann, Y. Tserkovnyak, G. S. D. Beach, E. E. Fullerton, C. Leighton, A. H. MacDonald, D. C. Ralph, D. A. Arena, H. A. Durr, P. Fischer, J. Grollier, J. P. Heremans, T. Jungwirth, A. V. Kimel, B. Koopmans, I. N. Krivorotov, S. J. May, A. K. Petford-Long, J. M. Rondinelli *et al.*, Rev. Mod. Phys. **89**, 025006 (2017).

[22] X. Jia, K. Liu, K. Xia, and G. E. W. Bauer, Europhys. Lett. **96**, 17005 (2011).

[23] G. Li, H. Jin, Y. Wei, and J. Wang, Phys. Rev. B **106**, 205303 (2022).

[24] P. Trocha and E. Siuda, Sci. Rep. **12**, 5348 (2022).

[25] T. Berlijn, P. C. Snijders, O. Delaire, H.-D. Zhou, T. A. Maier, H.-B. Cao, S.-X. Chi, M. Matsuda, Y. Wang, M. R. Koehler, P. R. C. Kent, and H. H. Weitering, Phys. Rev. Lett. **118**, 077201 (2017).

[26] Z. H. Zhu, J. Strempfer, R. R. Rao, C. A. Occhialini, J. Pelliciari, Y. Choi, T. Kawaguchi, H. You, J. F. Mitchell, Y. Shao-Horn, and R. Comin, Phys. Rev. Lett. **122**, 017202 (2019).

[27] S. W. Lovesey, D. D. Khalyavin, and G. van der Laan, Phys. Rev. B **105**, 014403 (2022).

[28] L. Šmejkal, R. Gonzalez-Hernandez, T. Jungwirth, and J. Sinova, Sci. Adv. **6**, eaaz8809 (2020).

[29] H. Bai, L. Han, X. Y. Feng, Y. J. Zhou, R. X. Su, Q. Wang, L. Y. Liao, W. X. Zhu, X. Z. Chen, F. Pan, X. L. Fan, and C. Song, Phys. Rev. Lett. **128**, 197202 (2022).

[30] S. Karube, T. Tanaka, D. Sugawara, N. Kadoguchi, M. Kohda, and J. Nitta, Phys. Rev. Lett. **129**, 137201 (2022).

[31] A. Bose, N. J. Schreiber, R. Jain, D.-F. Shao, H. P. Nair, J. Sun, X. S. Zhang, D. A. Muller, E. Y. Tsymbal, D. G. Schlom, and D. C. Ralph, Nat. Electron. **5**, 263 (2022).

[32] S. Das, D. Suri, and A. Soori, J. Phys.: Condens. Matter **35**, 435302 (2023).

[33] Q. Cui, B. Zeng, T. Yu, H. Yang, and P. Cui, arXiv:2306.08976.

[34] H. Bai, Y. C. Zhang, Y. J. Zhou, P. Chen, C. H. Wan, L. Han, W. X. Zhu, S. X. Liang, Y. C. Su, X. F. Han, F. Pan, and C. Song, Phys. Rev. Lett. **130**, 216701 (2023).

[35] L. Šmejkal, J. Sinova, and T. Jungwirth, Phys. Rev. X **12**, 040501 (2022).

[36] L. Šmejkal, A. B. Hellenes, R. Gonzalez-Hernandez, J. Sinova, and T. Jungwirth, Phys. Rev. X **12**, 011028 (2022).

[37] P. W. Anderson, Phys. Rev. **109**, 1492 (1958).

[38] E. Abrahams, P. W. Anderson, D. C. Licciardello, and T. V. Ramakrishnan, Phys. Rev. Lett. **42**, 673 (1979).

[39] G. Bergmann, Phys. Rev. B **28**, 2914 (1983).

[40] D. E. Khmel'nitskii, Physica B+C **126**, 235 (1984).

[41] S. Kobayashi and F. Komori, Prog. Theor. Phys. Suppl. **84**, 224 (1985).

[42] S. Hikami, A. I. Larkin, and Y. Nagaoka, Prog. Theor. Phys. **63**, 707 (1980).

[43] C. P. Umbach, S. Washburn, R. B. Laibowitz, and R. A. Webb, Phys. Rev. B **30**, 4048 (1984).

[44] P. A. Lee and A. D. Stone, Phys. Rev. Lett. **55**, 1622 (1985).

[45] B. L. Altshuler, JETP Lett. **41**, 648 (1985).

[46] P. A. Lee, A. D. Stone, and H. Fukuyama, Phys. Rev. B **35**, 1039 (1987).

[47] Y.-L. Han and Z.-H. Qiao, Front. Phys. **14**, 63603 (2019).

[48] P. Soven, Phys. Rev. **156**, 809 (1967).

[49] D. W. Taylor, Phys. Rev. **156**, 1017 (1967).

[50] B. Velický, Phys. Rev. **184**, 614 (1969).

[51] R. J. Elliott, J. A. Krumhansl, and P. L. Leath, Rev. Mod. Phys. **46**, 465 (1974).

[52] Y. Ke, K. Xia, and H. Guo, Phys. Rev. Lett. **100**, 166805 (2008).

[53] Y. Ke, K. Xia, and H. Guo, Phys. Rev. Lett. **105**, 236801 (2010).

[54] A. V. Kalitsov, M. G. Chshiev, and J. P. Velev, Phys. Rev. B **85**, 235111 (2012).

[55] Y. Zhu, L. Liu, and H. Guo, Phys. Rev. B **88**, 205415 (2013).

[56] J. Yan and Y. Q. Ke, Phys. Rev. B **94**, 045424 (2016).

[57] J. Yan, S. Wang, K. Xia, and Y. Ke, Phys. Rev. B **95**, 125428 (2017).

[58] B. Fu, L. Zhang, Y. Wei, and J. Wang, Phys. Rev. B **96**, 115410 (2017).

[59] C. Zhang, F. Xu, and J. Wang, Front. Phys. **16**, 33502 (2021).

[60] T. Holstein and H. Primakoff, Phys. Rev. **58**, 1098 (1940).

[61] J. C. Slater, Phys. Rev. **35**, 509 (1930).

[62] There is an extra factor $\sqrt{2S_0}$ associated with a_q and $a_q^\dagger$ in Hamiltonian which we dropped for the moment. Here S_0 is the length of the lattice spin.

[63] B. Velický, S. Kirkpatrick, and H. Ehrenreich, Phys. Rev. **175**, 747 (1968).

[64] K. Levin, B. Velický, and H. Ehrenreich, Phys. Rev. B **2**, 1771 (1970).

[65] Y. Zhu, L. Liu, and H. Guo, Phys. Rev. B **88**, 085420 (2013).

[66] J. N. Zhuang and J. Wang, J. Appl. Phys. **114**, 063708 (2013).

[67] C. Zhou, X. Chen, and H. Guo, Phys. Rev. B **94**, 075426 (2016).

[68] P. Sheng, *Introduction to Wave Scattering, Localization and Mesoscopic Phenomena* (Springer, New York, 2006).

[69] J. Ren, Phys. Rev. B **88**, 220406(R) (2013).

[70] G. M. Tang, X. Chen, J. Ren, and J. Wang, Phys. Rev. B **97**, 081407(R) (2018).

[71] L. Gu, H. H. Fu, and R. Wu, Phys. Rev. B **94**, 115433 (2016).

[72] M. P. Lopez-Sancho, J. M. Lopez-Sancho, and J. Rubio, J. Phys. F: Met. Phys. **14**, 1205 (1984); **15**, 851 (1985).

[73] J. S. Zheng, S. Bender, J. Armaitis, R. E. Troncoso, and R. A. Duine, Phys. Rev. B **96**, 174422 (2017).

[74] A. Brataas, Yu. V. Nazarov, and G. E. W. Bauer, Phys. Rev. Lett. **84**, 2481 (2000).

[75] G. Li, F. Xu, and J. Wang, Front. Phys. **18**, 33310 (2023).

[76] This is confirmed by the localization length study [75].